COMMUNICATIONS IN SCIENCE AND TECHNOLOGY
Homepage: cst.kipmi.or.id

Tunable copper oxide quantum dots: Electrochemical synthesis, characterization, and advanced applications

Supphadate Sujinnapram[a], Kampeepan Kengtone[a], Chainarong Raktham[b], Kritsada Hongsith[c,d], Supab Choopun[d], Sutthipoj Wongrerkdee[a,*]

[a]*Department of Physical and Material Sciences, Faculty of Liberal Arts and Science, Kasetsart University Kamphaeng Saen Campus, Nakhon Pathom 73140, Thailand*
[b]*Faculty of Education, Uttaradit Rajabhat University, Uttaradit 53000, Thailand*
[c]*Office of Research Administration, Chiang Mai University, Chiang Mai 50200, Thailand*
[d]*Department of Physics and Materials Science, Faculty of Science, Chiang Mai University, Chiang Mai 50200, Thailand*

Article history:
Received: 11 January 2025 / Received in revised form: 5 March 2025 / Accepted: 17 April 2025

Abstract

This work represents tunable copper oxide quantum dots (QDs) using an electrochemical synthesis in a mixture of electrolytes of citric acid (CA) and potassium chloride (KCl). The colloidal solutions showed a blue coloration, indicating quantum size effects and uniform dispersion of spherical QDs. The absorbance slightly decreased as the concentration of CA and KCl increased. PL studies indicated the maximum emission intensity at high CA and KCl concentrations due to great stabilization and surface-passivated quantum confinement effects. SAED confirmed polycrystalline structures of CuO and Cu_2O depending on the concentration of CA and KCl. This possibility of tuning particle size and crystalline phases offers significant potential for advanced applications. For a demonstration of the QDs as an antibacterial agent, it demonstrates potential as an agent for inhibiting *E. coli* and *S. aureus*. Furthermore, the integration of the QDs with ZnO-based photocatalysts resulted in an enhanced photocatalytic degradation of methylene blue.

Keywords: Copper oxide; quantum dots; electrochemical synthesis; antibacterial agent; photocatalytic degradation

1. Introduction

Quantum confinement in semiconducting materials is an important effect responsible for unique properties that enhance performance in advanced applications. Due to the quantum confinement effect, quantum dots (QDs) are of great interest because of their unique electrical and optical properties. QDs exhibit size-tunable emission wavelengths, high brightness, and stability; hence, they greatly serve in several applications, such as medical imaging, photovoltaics, light-emitting diodes, catalysis, sensors, and semiconducting inks [1-4]. QDs are versatile materials whose optical properties can be tuned based on several factors like shape, defects, crystalline, impurities, and size. All such factors can be controlled to a reasonable extent during their synthesis. QDs of CdE (E = S, Se, Te) are widely studied due to their precursor's availability, easy manipulation in aqueous solutions, and favorable band-gap energy (E_g), enabling emission across the whole visible spectrum [5-7]. The growth of the particles through atomic self-assembly is a simple method for obtaining size-controlled, water-soluble QDs, such as CdTe, by bottom-up wet-chemical reactions. In the synthesis, reaction mixtures containing precursors such as Cd^{2+} and Te^{2+} are prepared under controlled conditions. The reaction proceeds to the extent of the desired particle size, yielding an emission spectrum related to the particle structure.

Copper oxide represents a particularly interesting semiconductor since it is abundant and low cost, offering a competitive alternative to other expensive QD materials with lower abundance, such as CdSe or PbS, an important consideration for large-scale applications. In addition, copper oxide has low toxicity, gaining attention for environmental global concerns. Therefore, copper oxide QDs could become a promising area of research for technology sustainability. For example, Vaseem et al. [4] have demonstrated the synthesis of CuO QDs through a simple solution process. The as-synthesized QDs were highly crystalline in the monoclinic phase of CuO with an E_g of 1.75 eV and a diameter of 5-8 nm. These CuO QDs were further developed into ink suitable for inkjet printing applications, especially in the fabrication of CuO field-effect transistors (FETs). Electrical properties were

* Corresponding author.
Email: sutthipoj.s@gmail.com
https://doi.org/10.21924/cst.10.1.2025.1637

characterized by using CuO FETs fabricated by the inkjet-printed process in two distinct patterns: line and dot types. The resulting FETs showed a p-type semiconductor characteristic with a high carrier mobility for the line- and dot-patterned devices, respectively. In addition, microwave-assisted annealing in both patterns significantly increased carrier mobility, approximately two-fold higher. This investigation represents the highest mobility for p-type CuO FETs and therefore illustrates the potential of CuO QDs in advanced electronic applications. Similarly, Piri et al. [8] synthesized ultra-small CuO QDs using a precipitation method with the incorporation of surface modifiers such as PVP, Tween 80, and CTAB. The prepared CuO QDs exhibited several interesting features. They had a broad E_g between 2 and 2.5 eV, which was larger compared to bulk CuO. Additionally, the QDs were extremely small, with an average size of approximately 2.3 nm. This nanoscale size indicated the effect of quantum confinement. These properties demonstrate that the CuO QDs exhibit distinct electronic and optical behavior due to their QD structure.

This study focuses on electrochemical synthesis of copper oxide QDs. The synthesis was carried out at a constant applied voltage of 2 V for 6 hours in a mixed electrolyte of citric acid (CA) and potassium chloride (KCl) at varying proportions. The use of these electrolytes with such compositions has a dual function: CA acts as a complexing agent, influencing the morphology and stabilization of QDs, while KCl allows an increase in the conductivity of the electrolyte solution and facilitates the electrochemical reaction. For characterization, various techniques were used to analyze the copper oxide QDs, including an ultraviolet-visible spectrophotometer, photoluminescence spectrophotometer, transmission electron microscope, and selected area electron diffraction. To evaluate the applicable performance, the synthesized copper oxide QDs were used as an antibacterial agent to inhibit bacterial growth and integrated with ZnO photocatalysts to enhance photocatalytic degradation of methylene blue.

2. Materials and Methods

2.1. Electrochemical synthesis of copper oxide QDs

The pure copper rod serving as an electrode was cleaned through ultrasonic cleaning in acetone for 20 minutes. The rod was further cleaned in a mixed solution of isopropanol/DI water in equal volume. Then, the cleaned copper rod was dried using a nitrogen gas gun. After that, two rods were inserted into a beaker with 30 mL of electrolyte for the electrochemical synthesis of copper oxide QDs [9,10]. For processing details, a programmable DC power supply (RIGOL, DP-831A) was used to apply a constant voltage of 2 V between the two electrodes for 6 hours. The electrolyte was prepared from a mixture of CA (CA; $C_6H_8O_7 \cdot H_2O$, AR, RCI Labscan) and KCl (Ajax Finechem, AR). For studying the influence of CA or KCl, the mixed electrolyte was divided into two sets of variable concentrations. The first set was prepared by fixing KCl concentration at 0.10 M with varied CA concentrations of 0.10, 0.15, 0.20, and 0.25 M. This is for investigating the effect of CA concentration on the copper oxide QDs. In another set, which fixed the CA concentration at 0.10 M with varying concentrations of 0.10, 0.15, 0.20, and 0.25 M KCl.

2.2. Characterization of copper oxide QDs

The absorption spectra were investigated over a wavelength range of 250 to 1000 nm using an ultraviolet-visible (UV-Vis) spectrophotometer (Varian, Cary50) for copper oxide QD colloids in electrolytes. The photoluminescence (PL) spectrophotometer (Horiba Scientific, Fluoro Max+ Spectrofluorometer) was used to examine PL emission behavior. Transmission electron microscopy (TEM; JEOL, JEM-2100Plus) was conducted to study the shape, size, and distribution of copper oxide QDs. The crystalline structure was evaluated using selected area electron diffraction (SAED) analysis.

2.3. Applications of copper oxide QDs

For beneficial evaluation, the synthesized copper oxide QDs were used as an antibacterial agent and integrated with ZnO for photocatalyst application [11]. The inhibition rate of bacterial growth (*E. coli* and *S. aureus*) using copper oxide QDs as the agent was analyzed, according to the previous report [12]. Each bacterial strain was diluted in culture medium to an optical density at 600 nm (OD600) of 0.07-0.10. Then, the suspension solution (100 µl) was mixed with the synthesized copper oxide QDs (10 µl) for 24 hours. In another application of photocatalyst, copper oxide QDs were integrated with ZnO to improve photocatalytic performance. ZnO was conventionally prepared using precipitation as described previously [13]. Then, 1 g of ZnO was added into 10 mL of electrolyte solution containing copper oxide QD colloids and stirred at room temperature for 1 hour. ZnO with attached copper oxide QDs was then filtered and dried at 120°C for 1 hour. A methylene blue solution with an initial concentration of 1 mg/L was prepared, and 0.1 g of ZnO with attached copper oxide QDs was dispersed into 100 mL of the methylene blue solution. The mixture was kept in the dark for 30 minutes to ensure adsorption equilibrium, followed by UV light exposure to initiate the photocatalytic reaction. The degradation of methylene blue was analyzed by monitoring its absorbance using UV-Vis spectroscopy.

3. Results and Discussion

The synthesis of the copper oxide QDs was carried out at a constant applied voltage of 2 V in different mixing solutions of CA and KCl for 6 hours under electrochemical conditions. Fig. 1 shows a photograph of the solution containing colloidal copper oxide QDs. The appearance of blue coloration seen in the solution is a characteristic of the optical properties of copper oxide QDs, attributing the quantum size effects to the colloidal copper oxide QDs in both sets. For the solutions of different CA concentrations, Fig. 1(a), the solution becomes more transparent as the concentration of CA increases. This behavior may indicate better stabilization of QDs due to the higher concentration of CA acting as a stabilizer or capping agent [14,15]. Citric acid most probably plays a dual role as a reducing agent and a stabilizer in the synthesis of copper oxide QDs. It also leads to higher stabilization because the increased

concentration of CA causes aggregation reduction, so the solutions remain clearer. Thus, very small copper oxide QDs can be formed. In another set of different KCl concentrations with increasing concentrations of KCl, Fig. 1(b), a similar trend to the increasing concentrations of CA was observed. KCl could act as an electrolyte and thus impact the ionic strength of the medium, which could promote better dispersion of copper oxide QDs by reducing electrostatic repulsion and aggregation [16,17]. This behavior also causes small-sized copper oxide QDs. Therefore, an increase in the concentrations of CA or KCl significantly changes the stability and dispersion of copper oxide QDs.

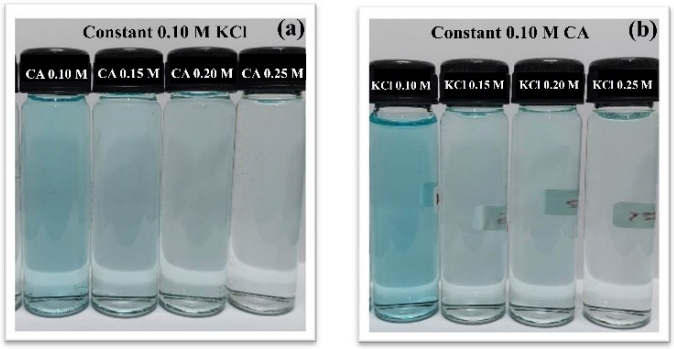

Fig. 1. Photograph of colloidal copper oxide QD suspension in a mixture of CA and KCl: (a) different CA concentrations; (b) different KCl concentrations

The investigation of absorption was performed using a UV-Vis spectrophotometer in the range of 250-1000 nm, as depicted in Fig. 2. The absorbance shows broad peaks in the wavelength region of around 800 nm, whose intensities decrease with increasing concentrations of both CA and KCl. The increase in the concentrations of either CA or KCl resulted in a marked decrease in absorbance, along with a gradual decrease in color intensity, as seen in the photographs (Fig. 1). The higher absorbance of lower concentrations indicates the higher concentrations of QDs with larger particle sizes. Conversely, the QDs exhibit high stability due to reduced aggregation at the lower absorbance.

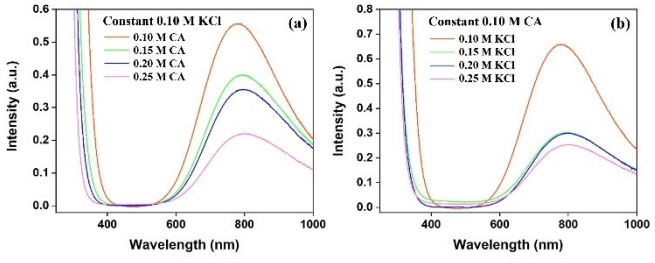

Fig. 2. Absorbance spectrum of colloidal copper oxide QD suspension in a mixture of CA and KCl: (a) different CA concentrations; (b) different KCl concentrations

While higher CA or KCl concentrations reduced particle aggregation as demonstrated by the decreased intensity and broader peaks of the absorbance, the optical properties of copper oxide QDs strongly depended on the concentration of CA and KCl, since the size, dispersion, and stabilization of particles are affected. Fig. 3 presents the PL emission of copper oxide QDs under excitation at 280 nm for various concentrations of CA or KCl. In addition, PL emission peaks for the different concentrations of CA are found to lie in the range of 399-419 nm, while the emission peaks corresponding to the different KCl concentrations tend to be around 402-409 nm [18,19]. The PL intensity increases with higher concentrations of CA and KCl, reaching a maximum at 0.25 M for both sets. This trend thus implies that higher concentrations of CA or KCl enhance stabilization and surface passivation of copper oxide QDs, resulting in fewer surface defects. The strong PL for 0.25 M CA or KCl may indicate the optimum stabilization conditions for QDs, which in turn increased quantum yield. The peak performance could suggest a fine balance in surface chemistry, quantum confinement effects, and particle size uniformity, which are all crucial factors toward maximizing the optical properties of QDs. The behavior can be described as CA acting as a capping agent upon binding to the QD surface, preventing QD aggregation, improving colloidal stability, and reducing non-radiative recombination pathways. The ionic stabilization by KCl assists in a homogenous distribution of QDs in solutions, further improving surface chemistry. Thus, the synthesized copper oxide QDs could be optimized by the synergy of CA and KCl, resulting in more perfect particles with better-defined optical properties.

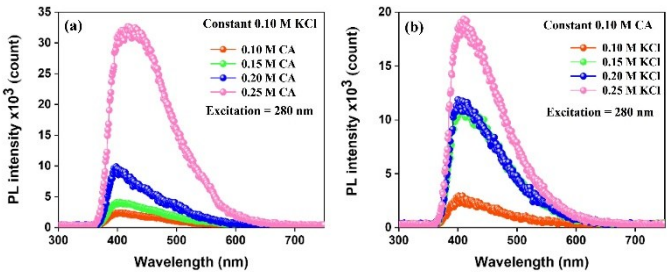

Fig. 3. PL emission of colloidal copper oxide QD suspension in a mixture of CA and KCl: (a) different CA concentrations; (b) different KCl concentrations

High-resolution TEM (HR-TEM) was used to study the nature of copper oxide QDs, as depicted in Fig. 4. The middle-range concentration conditions were chosen for analysis, such as 0.10 M KCl/0.15 M CA, 0.10 M KCl/0.20 M CA, 0.10 M CA/0.15 M KCl, and 0.10 M CA/0.20 M KCl. The HR-TEM images show that the copper oxide QDs were well-dispersed with small spherical size, measuring less than 10 nm across all selected samples. Further analysis using Image-J software was performed on selected clear HR-TEM images, namely Fig. 4(a,d), as presented in Fig. 5. This further investigation gave the size of the particles, and the average diameter was 1.66 ± 0.33 nm for QDs synthesized with 0.10 M KCl/0.15 M CA and 2.11 ± 0.45 nm for those prepared with 0.10 M CA/0.20 M KCl. These results confirm that the sizes of the copper oxide QDs are well below the 5 nm, qualifying them as QDs. The dimensions lower than 5 nm are significant for ensuring the effects of quantum confinement that play a crucial role in the optical and electronic properties of the QDs [20,21]. These results imply the precision of the synthesis toward the production of size-controlled QDs with improved uniformity and functional properties.

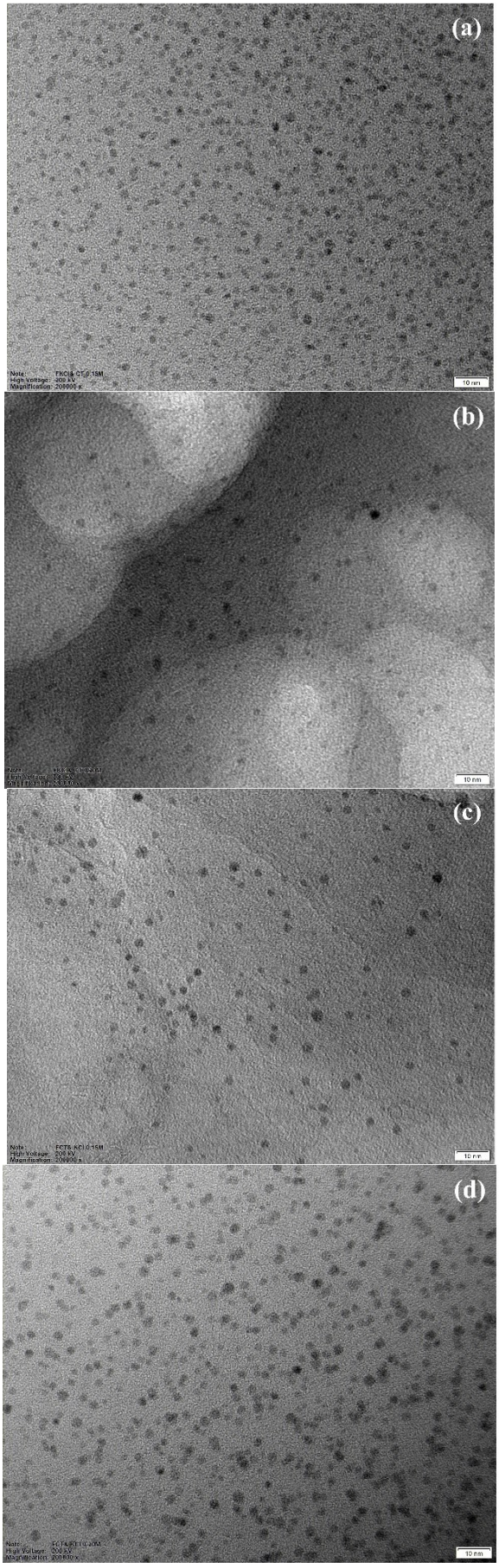

Fig. 4. HR-TEM images of copper oxide QDs prepared at different conditions: (a) 0.10 M KCl/0.15 M CA; (b) 0.10 M KCl/0.20 M CA; (c) 0.10 M CA/0.15 M KCl; (d) 0.10 M CA/0.20 M KCl

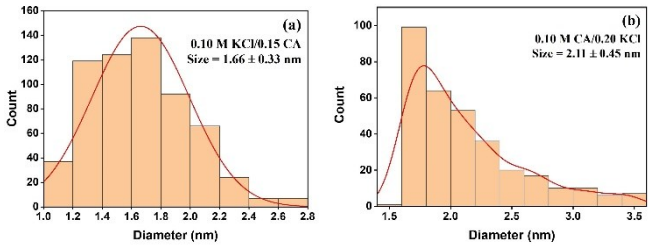

Fig. 5. Distribution of particle's diameter of copper oxide QDs prepared at different: (a) 0.10 M KCl/0.15 M CA; (b) 0.10 M CA/0.20 M KCl

Meanwhile, SAED was also performed for the crystalline investigation of copper oxide QDs, which were electrochemically prepared in mixed solutions of 0.10 M KCl/0.15 M CA and 0.10 M CA/0.20 M KCl, as shown in Fig. 6. The ring-like diffraction patterns were found in both cases, revealing a characteristic of polycrystalline structures. These ring-like features imply that the copper oxide QDs are composed of numerous crystalline grains, randomly oriented due to the stochastic nature of the crystallization during synthesis. SAED patterns of copper oxide QDs were matched with standard references to identify their crystalline phases. The results showed that QDs corresponded to CuO and Cu_2O [22-24], depending on the relative concentrations of CA and KCl used in the synthesis. Consequently, it can be concluded that a higher CA concentration tends to produce CuO, whereas a high concentration of KCl favors the Cu_2O formation. These results suggest synthesis conditions causing changes in copper oxide QD crystalline phases.

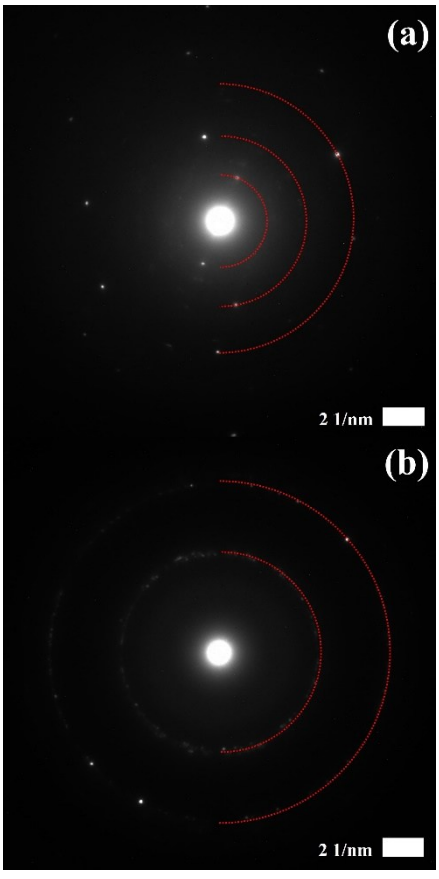

Fig. 6. SAED patterns of copper oxide QDs prepared at different conditions: (a) 0.10 M KCl/0.15 M CA; (b) 0.10 M CA/0.20 M KCl

In this view, the polycrystalline nature can provide significant insight into the possible applications of these QDs [25]. Often, a high grain boundary area is believed to result in surface activity, supporting several applications such as antibacterial agents and catalysis [26-28]. Thus, the CuO and Cu_2O QDs were used to demonstrate a beneficial application as antibacterial agents against *E. coli* and *S. aureus*. The inhibition rate of CuO and Cu_2O QDs was calculated [12,29]. The inhibition rate for *E. coli* and *S. aureus* under CuO QD agent is 32.11% and 33.12%, respectively, which are comparable antibacterial effects against both Gram-negative (*E. coli*) and Gram-positive (*S. aureus*) bacteria. The Cu_2O QDs exhibit higher inhibition rates (48.32% for *E. coli* and 48.62% for *S. aureus*) than CuO QDs. The similarity in inhibition rates for both bacterial strains indicates that the antibacterial activity of both QDs is not significantly influenced by bacterial cell wall differences. However, the findings suggest the potential of QDs as applicable antibacterial agents.

In photocatalyst improvement, the CuO and Cu_2O QDs were integrated with ZnO to form ZnO/CuO QDs and ZnO/Cu_2O QDs for enhancement of photocatalytic degradation of MB. Fig. 7 illustrates that the absorbance of MB gradually decreases with increasing UV irradiation time in the presence of all photocatalysts (ZnO, ZnO/CuO QDs, and ZnO/Cu_2O QDs), indicating the effective photocatalytic degradation of MB molecules. For quantitative evaluation of the photocatalytic performance, the degradation rate constant (k_r) for each condition was calculated according to the pseudo-first-order kinetics in Equation (1) [30-32], with the slope of the linear fit in Fig. 8 used to determine the k_r [33].

$$\mathrm{Ln}\,(A_t/A_0) = -k_r\,t \qquad (1)$$

where A_t and A_0 are absorbance intensity at interval and initial times, respectively, t is irradiation time. The k_r values were 7.03×10^{-3} min^{-1}, 7.47×10^{-3} min^{-1}, and 13.31×10^{-3} min^{-1} for ZnO, ZnO/CuO QDs, and ZnO/Cu_2O QDs, respectively. These results demonstrate a significant enhancement in the photocatalytic performance of ZnO when integrated with copper oxide QDs. In comparison of ZnO/CuO and ZnO/Cu_2O structures, the ZnO/Cu_2O exhibits greater photocatalytic performance. This behavior may be attributed to charge transfer mechanisms governed by different energy band alignments [34-36], as illustrated in Fig. 9. After photoactivation, electrons and holes are generated at the conduction band (CB) and valence band (VB), respectively. For the ZnO/CuO in Fig. 9(a), electrons and holes of ZnO possibly transfer to the CB and VB of CuO, respectively. This process causes high charge carrier density and accelerates recombination at CuO, which reduces charge carriers for photocatalysis. For the ZnO/Cu_2O in Fig. 9(b), the transfer of electrons from CB of Cu_2O to CB of ZnO and holes from VB of ZnO to VB of Cu_2O are allowed, which leads to effective charge separation and extends the lifetime for charge interaction with surrounding molecules during photocatalytic activity. Thus, ZnO/Cu_2O explores excellent photocatalytic degradation of MB. These findings demonstrate the critical role of band alignment in optimizing the photocatalytic activity of ZnO integrated with copper oxide QDs.

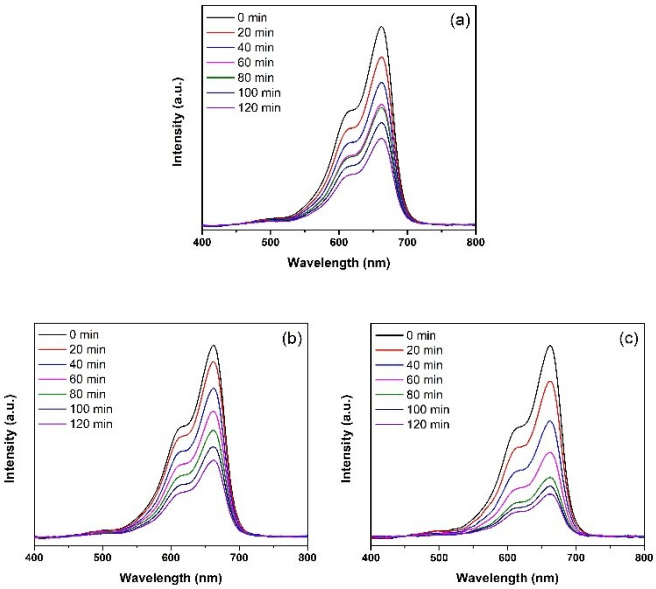

Fig. 7. Absorbance of MB after photocatalytic degradation using different photocatalysts: ZnO; (b) ZnO/CuO QDs; (c) ZnO/Cu_2O QDs

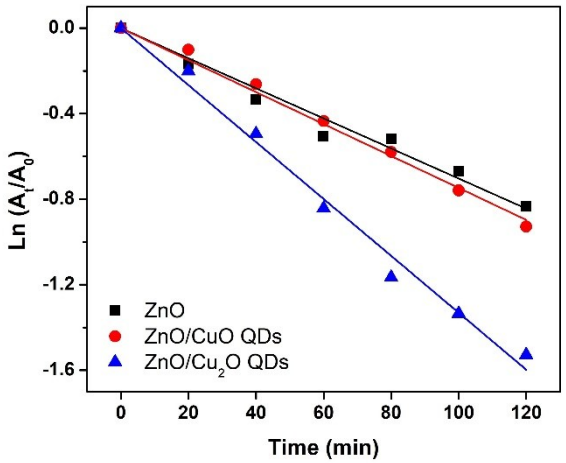

Fig. 8. Degradation rate constant analysis for photocatalytic degradation of MB using ZnO, ZnO/CuO QDs, and ZnO/Cu_2O QDs

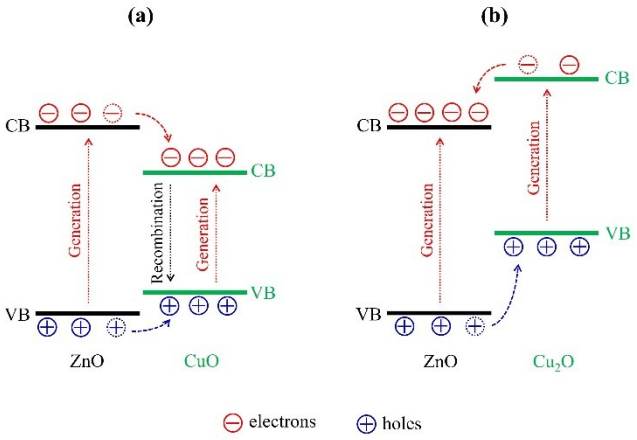

Fig. 9. Schematic illustration of energy band alignment of (a) ZnO/CuO and (b) ZnO/Cu_2O

4. Conclusion

Copper oxide QDs were synthesized via an electrochemical method with well-controlled parameters: the applied voltage was kept constant at 2 V for 6 hours. The characteristic blue coloration of the colloidal solutions reflects typical quantum size effects of the synthesized QDs, underlining the success of the preparation method. From the UV-Vis spectra, it was observed that with increasing concentration of CA or KCl, the intensity of absorbance decreased while peaks broadened, implying the increased stability and reduced aggregation of QDs. The PL analysis showed that 0.25 M CA or KCl had an optimal stabilization condition in which QDs exhibited maximum PL intensity, indicative of higher quantum yield and efficient surface passivation. Structural characterizations showed the synthesis of well-dispersed spherical QDs. Controllable particle sizes below 5 nm were tuned by CA and KCl concentrations, indicating the flexibility of the electrochemical synthesis approach. The SAED patterns revealed that the synthesized QDs had polycrystalline structures with ring-like diffraction patterns. These were identified to be CuO and Cu_2O phases whose formation depended on the relative concentrations of CA and KCl. For beneficial applications, the CuO and Cu_2O QDs exhibit potential as antibacterial agents for inhibiting *E. coli* and *S. aureus*. Furthermore, the integration of CuO and Cu_2O QDs with ZnO results in a significant improvement in the photocatalytic performance for MB degradation, especially Cu_2O QDs. This work demonstrates that electrochemical synthesis of copper oxide QDs by controlling CA and KCl concentration is a versatile and efficient method to produce stable QDs with controlled size, excellent optical, and structural properties for suitable applications.

Acknowledgements

This work was funded by the Faculty of Liberal Arts and Science, Kasetsart University Kamphaeng Saen Campus (Grant no. 305/2567). The authors also acknowledge the Faculty of Education, Uttaradit Rajabhat University; and the Department of Physics and Materials Science, Faculty of Science, Chiang Mai University for valuable support in providing partial materials and access to analytical equipment, which significantly contributed to the success of this study.

References

1. B. A. Kumar, T. Elangovan, D. Karthigaimuthu, D. Aravinth, G. Ramalingam, F. Ran, S. Sangaraju, *CdSe Quantum Dots Bedecked on ZnO/TiO_2/CuO Ternary Nanocomposite for Enhanced Photocatalytic and Photovoltaic Applications*, Langmuir 39 (2023) 15864-15877.
2. X. Yuan, L. Meng, Z. Xu, C. Zheng and H. Zhao, *CuO Quantum Dots Supported by $SrTiO_3$ Perovskite Using the Flame Spray Pyrolysis Method: Enhanced Activity and Excellent Thermal Resistance for Catalytic Combustion of CO and CH_4*, Environ. Sci. Technol. 55 (2021) 14080-14086.
3. A. Mirzaei, Z. Kordrostami, M. Shahbaz, J.Y. Kim, H.W. Kim, S.S. Kim, *Resistive-Based Gas Sensors Using Quantum Dots: A Review*. Sensors 22 (2022) 4369.
4. M. Vaseem, A.R. Hong, R.T. Kim, Y. B. Hahn, *Copper oxide quantum dot ink for inkjet-driven digitally controlled high mobility field effect transistors*, J. Mater. Chem. C 1 (2013) 2112-2120.
5. F. Ebrahim, O. Al-Hartomy, S. Wageh, *Cadmium-Based Quantum Dots Alloyed Structures: Synthesis, Properties, and Applications*. Materials 16 (2023) 5877.
6. N.A. Akil, S.D. Guo, *Lattice Thermal Transport of BAs, CdSe, CdTe, and GaAs: A First Principles Study*. J. Electron. Mater. 52 (2023) 3401-3412.
7. J. Yang and X. Zhong, *CdTe based quantum dot sensitized solar cells with efficiency exceeding 7% fabricated from quantum dots prepared in aqueous media*, J. Mater. Chem. A 4(2016) 16553-16561.
8. F. Piri, M.S. Afarani, A.M. Arabi, *Synthesis of copper oxide quantum dots: effect of surface modifiers*, Mater. Res. Express 6 (2019) 125006.
9. R. Panyathip, T. Sintiam, S. Weerapong, A. Ngamjarurojana, P. Kumnorkaew, S. Choopun, S. Sucharitakul, *Electrolytic effect on growth of graphene quantum dots via electrochemical process*, Surf. Rev. Lett. 28 (2021) 2150117.
10. R. Panyathip, S. Sucharitakul, S. Phaduangdhitidhada, A. Ngamjarurojana, P. Kumnorkaew, S. Choopun, *Surface Enhanced Raman Scattering in Graphene Quantum Dots Grown via Electrochemical Process*. Molecules 26 (2021) 5484.
11. N. Munandar, S. Kasim, R. Arfah, D.N. Basir, Y. Hala, M. Zakir, H. Natsir, *Green synthesisof copper oxide (CuO) nanoparticles using Anredera cordifolialeaf extract and their antioxidant activity*, Commun. Sci. Technol. 7 (2022) 127–134
12. S. Krobthong, S. Wongrerkdee, *Incorporation of Fe and Cu for antibacterial performance enhancement of Fe-Cu-ZnO nanocomposites synthesized by a facile chemical precipitation*, J. Met. Mater. Miner. 30 (2020) 38-45.
13. T. Rungsawang, S. Krobthong, K. Paengpan, N. Kaewtrakulchai, K. Manatura, A. Eiad-Ua, C. Boonruang, S. Wongrerkdee, *Synergy of functionalized activated carbon and ZnO nanoparticles for enhancing photocatalytic degradation of methylene blue and carbaryl*, Radiat. Phys. Chem. 223 (2024) 111924.
14. A. Omelyanchik, F. G. da Silva, G. Gomide, I. Kozenkov, J. Depeyrot, R. Aquino, A.F.C. Campos, D. Fiorani, D. Peddis, V. Rodionova, S. Jovanović, *Effect of citric acid on the morpho-structural and magnetic properties of ultrasmall iron oxide nanoparticles*, J. Alloys Compd. 883 (2021) 160779.
15. M. Bai, W. Li, H. Yang, W. Dong, Q. Wang, Q. Chang, *Morphology-controlled synthesis of MoS_2 using citric acid as a complexing agent and self-assembly inducer for high electrochemical performance*, RSC Adv. 12 (2022) 28463-28472.
16. C. Pizarro, M. Escudey, C. Bravo, M. Gacitua and L. Pavez, *Sulfate Kinetics and Adsorption Studies on a Zeolite/Polyammonium Cation Composite for Environmental Remediation*, Minerals 11 (2021) 180.
17. D.H. Song, Y.K. Ham, S.W. Noh, K.B. Chin, H.W. Kim, *Evaluation of NaCl and KCl Salting Effects on Technological Properties of Pre- and Post-Rigor Chicken Breasts at Various Ionic Strengths*, Foods 9 (2020) 721.
18. P. Kar, M.K. El-Tahlawy, Y. Zhang, M. Yassin, N. Mahdi, R. Kisslinger, U.K. Thakur, A.M. Askar, R. Fedosejevs, K. Shankar, *Anodic copper oxide nanowire and nanopore arrays with mixed phase content: synthesis, characterization and optical limiting response*, J. Phys. Commun. 1 (2017) 045012.
19. Z. Hu, Y. Tang, Z. Yue, W. Zheng, Z. Xiong, *The facile synthesis of copper oxide quantum dots on chitosan with assistance of phyto-angelica for enhancing the human osteoblast activity to the application of osteoporosis*, J Photochem. Photobiol. B 191 (2019) 6-12.

20. G. Liu, W. Liang, X. Xue, F. Rosei, Y. Wang, *Atomic Identification of Interfaces in Individual Core@shell Quantum Dots*, Adv. Sci. 8 (2021) 2102784.
21. S. Hao, S. Suebka, J. Su, *Single 5-nm quantum dot detection via microtoroid optical resonator photothermal microscopy*, Light Sci. Aappl. 13 (2024) 195.
22. F. Peng, Y. Sun, Y. Lu, W. Yu, M. Ge, J. Shi, R. Cong, J. Hao, N. Dai, *Studies on Sensing Properties and Mechanism of CuO Nanoparticles to H_2S Gas*. Nanomaterials 10 (2020) 774.
23. D. Huo, W. Liu, *Controlled synthesis of Cu_2O nanorods in aqueous solution using gallic acid as both reductant and crystal growth modifier*, Catal. Commun. 170 (2022) 106494.
24. Y. Li, X. Chen, L. Li, *Facile thermal exfoliation of Cu sheets towards the CuO/Cu_2O heterojunction: a cost-effective photocatalyst with visible-light response for promising sustainable applications*, RSC Adv. 9 (2019) 33395-33402.
25. S. Krobthong, K. Umma, T. Rungsawang, T. Mirian, S. Wongrerkdee, S. Nilphai, K. Hongsith, S. Choopun, S. Wongrerkdee, C. Raktham, P. Pimpang, *Synthesis and characterization of Cu_2O and CuO nanoparticles in distilled water using electrochemical process*, Dig. J. Nanomater. Bios. 20 (2025) 13-21.
26. Y. Chen, X. Wang, Z. Zeng, M. Lv, K. Wang, H. Wang, X. Tang, *Towards molecular understanding of surface and interface catalytic engineering in TiO_2/$TiOF_2$ nanosheets photocatalytic antibacterial under visible light irradiation*, J. Hazard. Mater. 465 (2024) 133429.
27. A. Menichetti, A. Mavridi-Printezi, D. Mordini, M. Montalti, *Effect of Size, Shape and Surface Functionalization on the Antibacterial Activity of Silver Nanoparticles*. J. Funct. Biomater. 14 (2023) 244.
28. A. Ramasubramanian, V. Selvaraj, P. Chinnathambi, S. Hussain, D. Ali, G. Kumar, P. Balaji, S. Sagadevan, *Enhanced photocatalytic degradation of methylene blue from aqueous solution using green synthesized ZnO nanoparticles*. Biomass Conv. Bioref. 13 (2023) 17271-17282.
29. Y.P. Wu, X.Y. Liu, J.R. Bai, H.C. Xie, S.L. Ye, K. Zhong, Y.N. Huang, H. Gao, *Inhibitory effect of a natural phenolic compound, 3-p-trans-coumaroyl-2-hydroxyquinic acid against the attachment phase of biofilm formation of Staphylococcus aureus through targeting sortase A*, RSC Adv. 9 (2019) 32453-32461.
30. S. Krobthong, T. Rungsawang, N. Khaodara, N. Kaewtrakulchai, K. Manatura, K. Sukiam, D. Wathinputthiporn, S. Wongrerkdee, C. Boonruang, S. Wongrerkdee, *Sustainable Development of ZnO Nanostructure Doping with Water Hyacinth-Derived Activated Carbon for Visible-Light Photocatalysis*, Toxics 12 (2024) 165.
31. S. Sujinnapram, S. Krobthong, S. Moungsrijun, C. Boonruang, N. Kaewtrakulchai, A. Eiad-Ua, K. Manatura, S. Wongrerkdee, *A novel photocatalyst of Y_2O_3-BaO-ZnO ternary system for enhanced photocatalytic degradation of carbofuran insecticide*, Mater. Today Commun. 40 (2024) 109501.
32. S. Wongrerkdee, S. Wongrerkdee, C. Boonruang, S. Sujinnapram, *Enhanced Photocatalytic Degradation of Methylene Blue Using Ti-Doped ZnO Nanoparticles Synthesized by Rapid Combustion*, Toxics 11 (2023) 33.
33. F. Sa'adah, H. Sutanto, H. Hadiyanto, I. Alkian, *Efficient removal of amoxicillin, ciprofloxacin, and tetracycline from aqueous solution by Cu-Bi_2O_3 synthesized using precipitation-assisted-microwave*, Commun. Sci. Technol. 9 (2024) 170-178.
34. H. Yoo, S. Kahng, J.H. Kim, *Z-scheme assisted ZnO/Cu_2O-CuO photocatalysts to increase photoactive electrons in hydrogen evolution by water splitting*, Sol. Energy Mater. Sol. Cells, 204 (2020) 110211.
35. B. Uma, K.S. Anantharaju, L. Renuka, H. Nagabhushana, S. Malini, S.S. More, Y.S. Vidya, S. Meena, *Controlled synthesis of (CuO-Cu_2O)Cu/ZnO multi oxide nanocomposites by facile combustion route: A potential photocatalytic, antimicrobial and anticancer activity*, Ceram. Int. 47 (2021) 14829-14844.
36. N. Subha, M. Mahalakshmi, M. Myilsamy, B. Neppolian, V. Murugesan, *Direct Z-scheme heterojunction nanocomposite for the enhanced solar H_2 production*, Appl. Catal. A: Gen. 553 (2018) 43-51.